Biol. Cybern. 69, 257–267 (1993)

Biological Cybernetics

A computational study of the effects of serotonin on a molluscan burster neuron

Richard Bertram*

Department of Mathematics and Supercomputer Computations Research Institute, Florida State University, Tallahassee, FL 32306-4052, USA

Received: 4 December 1992/Accepted in revised form: 18 January 1993

Abstract. A mathematical model of burster neuron R_{15} from the abdominal ganglion of *Aplysia* is presented. This is an improvement over earlier models in that the bursting mechanism is more accurately represented. The improved model allows for simulated application of the neurotransmitter serotonin, which has been reported to have profound effects on the voltage waveform produced by R_{15}. Computational analysis indicates that the serotonin-induced modulation of the waveform can be explained in terms of competition between stationary, bursting, and beating attractors. Analysis also indicates that, as a result of this competition, serotonin increases the sensitivity of the neuron to synaptic perturbations. This may have important consequences with regard to water balance in the *Aplysia*, particularly during egg laying.

1 Introduction

Neuron R_{15}, located in the abdominal ganglion of the marine mollusk *Aplysia*, has been the topic of investigation for over 20 years (e.g., Mathieu and Roberge 1971; Gorman et al. 1982; Adams and Benson 1985). This is due primarily to the complex electrical bursting oscillation, consisting of a burst of action potentials followed by a quiescent period of membrane hyperpolarization, generated endogenously by the neuron (Fig. 1). Early studies (Junge and Stephens 1973; Smith 1980; Gorman et al. 1982) suggested that the bursting oscillation is generated by an inactivating potassium current, but more recent work has suggested a different mechanism.

Two small excitatory ionic currents, I_{NSR} and I_D, have been characterized in several voltage clamp studies (Lewis 1984; Adams 1985; Adams and Levitan 1985). This work has led to the proposal of a mechanism for the generation of bursting based on the interaction of these currents (Adams and Benson 1985; Adams and Levitan 1985). According to this proposal, I_{NSR} initiates the burst and then inactivates as calcium ions accumulate inside the cell. The inactivation of this current ultimately terminates the burst. Excitatory current I_D increases from zero with the first spike and grows throughout the early portion of the burst. It is responsible for maintaining the burst and produces, following the last spike, the depolarizing after-potential (DAP). This is the characteristic voltage "hump" following each burst of spikes in R_{15}.

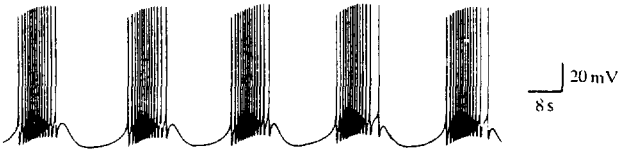

Fig. 1. Laboratory recording of R_{15} bursting waveform. Reprinted with permission from Lotshaw et al. (1986)

Several mathematical models have been described previously that exhibit some form of bursting. These range from the simple model of Hindmarsh and Rose (1984) to the more complex models of Plant and Kim (1975) and Plant (1978). Although these models generate a bursting oscillation, they do not make use of the ionic mechanism (described above) that is now thought to be responsible for the oscillation in R_{15}. The plausibility of this mechanism is tested in Adams and Benson (1985), but the model described there does not include a calcium-inactive subthreshold current.

In the first part of this paper a mathematical model is described which employs a more accurate representation of the R_{15} bursting mechanism. Models for the ionic currents I_{NSR} and I_D are included as well as the other major ionic currents known to exist in the axon hillock region of the neuron. All system parameters are set in accordance with published experimental data. The voltage waveform generated by this model is seen to exhibit all the major characteristics of the actual R_{15} waveform, some of which were not seen with earlier models.

Next, the R_{15} model is used to investigate the effects of external application of the neurotransmitter sero-

*Present address: Mathematical Research Branch, NIDDK, NIH, Bethesda, MD 20892, USA

tonin (5-hydroxytryptamine), a neurotransmitter found in both invertebrates and vertebrates. Experiments have shown that application of varying concentrations of serotonin causes the burst to be enhanced or terminated or transformed into a beating oscillation consisting of a continuous sequence of voltage spikes (Drummond et al. 1980; Levitan and Levitan 1988). The effects of serotonin typically last for several hours. One goal of the present computational study is to foster a better understanding of the manner in which this modulation is brought about.

Serotonin acts on R_{15} by increasing the intracellular concentration of the second messenger cyclic AMP, which in turn increases the conductance of two opposing subthreshold currents, I_{NSR} and I_R (Drummond et al. 1980; Benson and Levitan 1983; Lotshaw et al. 1986; Levitan and Levitan 1988). Similar effects are produced by external application of egg-laying hormone, which is released during egg laying from two clusters of neuroendocrine cells known as bag cells (Mayeri et al. 1985; Levitan et al. 1987). During egg laying, these cells fire for up to 40 min (Kandel 1979), secreting egg-laying hormone as well as other hormones that diffuse throughout the abdominal ganglion. Thus, the waveform modulation induced by exogenous application of serotonin or egg-laying hormone is representative of conditions prevailing during egg laying.

The actions of serotonin are modeled here by increasing the maximum conductance of I_{NSR} and an inward-rectifying potassium current I_R in a manner described by published data. Computational analysis of this model indicates that the bursting oscillation persists for low serotonin concentration levels, followed for higher concentration levels by a bistable region in which a stable periodic beating oscillation and a stable stationary solution coexist. The relative "strength" of these attracting solutions changes as the serotonin concentration is increased, yielding the different waveforms seen in the laboratory.

In the final portion of the paper the effects of synaptic perturbations are considered following the application of various concentrations of serotonin. This analysis indicates that in addition to its role in modulating the R_{15} waveform, serotonin sensitizes the neuron to synaptic input. R_{15} is a secretory cell which secretes osmoregulatory hormone with each voltage spike. Hence, by sensitizing the neuron to synaptic input, serotonin strengthens the coupling between the electrical activity of neurons synapsing onto R_{15} and salt intake through the skin of the animal. The topic of synaptic perturbations to serotonin-modulated R_{15} is taken up in more detail in a forthcoming paper (Bertram, in preparation).

2 The R_{15} model

The ionic currents included in the R_{15} model represent those found in the neuron's axon hillock region. They fall into two classes. *Spike* currents (I_{spike}) are those which contribute to the formation and shape of the action potential but have little effect on the initiation, maintenance, or termination of the bursting oscillation. *Subthreshold* currents (I_{sub}) are relatively small and have little effect on the action potential. However, they are active at voltages in which the spike currents are inactive and are thus responsible for driving the bursting oscillation. The rate of change of membrane potential or voltage is

$$\frac{dV}{dt} = -(I_{spike} + I_{sub} - I_{app})/C_M \tag{1}$$

where C_M is the membrane capacitance and I_{app} is any externally applied current. In the present model the mathematical form of individual ionic currents, as well as system parameters, is based on published data. The values of all parameters are given in Appendix A.

2.1 Spike currents

Classical currents. The classic spike currents described by Hodgkin and Huxley (1952) are present in the R_{15} hillock. The sodium current, I_{Na}, is largely responsible for the action potential upstroke and undergoes rapid voltage-dependent inactivation. The "delayed rectifying" potassium current, I_{K1}, aids in voltage repolarization following the peak of the action potential and undergoes slow voltage-dependent inactivation. Finally, a small leak current, I_l, is generated partly by the flow of chloride ions across the membrane. For details on these currents see Thompson (1977), Adams and Gage (1979a,b), and Adams and Benson (1985).

The sodium and delayed rectifying potassium currents are modeled here according to the Adams–Benson formulation (Adams and Benson 1989), and the model for the leak current is standard

$$I_{Na} = \bar{g}_{Na} m^3 h (V - V_{Na}) \tag{2}$$

$$I_{K1} = \bar{g}_{K1} n^2 j (V - V_K) \tag{3}$$

$$I_l = \bar{g}_l (V - V_l) \tag{4}$$

Here $V_{Na} = 55$ mV, $V_K = -75$ mV, and $V_l = -40$ mV are equilibrium potentials for the specific ions, m and n are activation variables, and h and j are fast and slow inactivation variables, respectively. The maximum conductance of each current is denoted by $\bar{g}$.

The activation and inactivation variables change with time according to

$$\frac{dm}{dt} = [m_\infty(V) - m]/\tau_m(V) \tag{5}$$

$$\frac{dn}{dt} = [n_\infty(V) - n]/\tau_n(V) \tag{6}$$

$$\frac{dh}{dt} = [h_\infty(V) - h]/\tau_h(V) \tag{7}$$

$$\frac{dj}{dt} = [j_\infty(V) - j]/\tau_j(V) \tag{8}$$

where the steady-state or infinity functions and time constants are shown in Figs. 2 and 3, respectively. Analytical expressions for these, as well as all other infinity and time constant functions, are given in Appendix A.

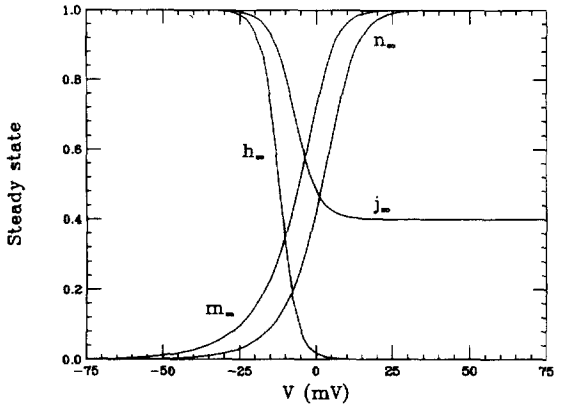

Fig. 2. Model steady-state activation and inactivation functions

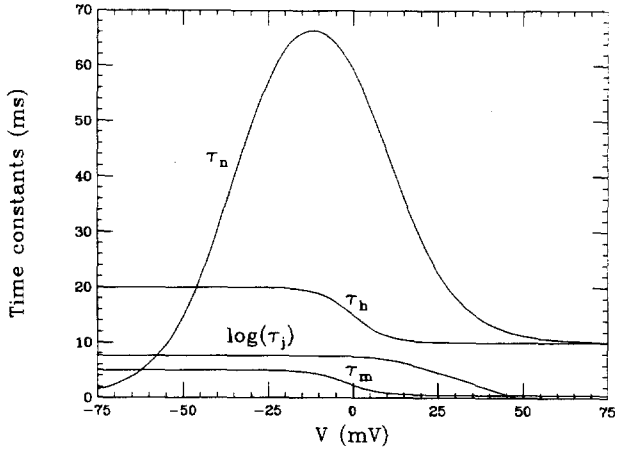

Fig. 3. Model activation and inactivation time constants

Additional spike currents. Besides the classic spike currents, a calcium current and a second potassium current are known to exist in and near the R_{15} hillock region. The excitatory calcium current, I_{Ca}, contributes to the spike upstroke and broadens the action potential. Perhaps its most important role is to bring calcium ions into the neuron which affect one of the small subthreshold currents, as described below. The second potassium current, I_{K2}, has kinetics and voltage dependence similar to those of I_{K1} and thus aids in repolarization after the action potential peak. For details on these two currents see Adams and Gage (1979a,b), Hille (1984), and Adams and Benson (1985).

Calcium activation is best described by a second power relation (Byerly and Hagiwara 1982), so calcium current is modeled here as

$$I_{Ca} = \bar{g}_{Ca} x^2 (V - V_{Ca}) \tag{9}$$

where $V_{Ca} = 100$ mV and x is the activation variable. This variable changes with time as

$$\frac{dx}{dt} = [x_\infty(V) - x]/\tau_x(V) \tag{10}$$

where the infinity and time constant functions are based on measurements made by Adams and Gage (1979a,b) and Adams and Benson (1985). These functions are similar to those of the sodium activation variable and so are not illustrated.

The potassium current I_{K2} is activated by intracellular calcium ions. Earlier models of this current (Plant 1978; Chay and Keizer 1983; Rinzel and Lee 1987), often referred to as $I_{K(Ca)}$, take the form

$$I_{K2} = \frac{\bar{g}_{K2} c}{(\bar{\mu}_\infty + c)} (V - V_K) \tag{11}$$

where c denotes the intracellular calcium ion concentration and $\bar{\mu}_\infty$ is a constant. This assumes that conductance, $\bar{g}_{K2} c/(\bar{\mu}_\infty + c)$, depends only on calcium concentration and not voltage. There is clear evidence, however, for voltage dependence in the ion channels (Gorman and Thomas 1980; Barrett et al. 1982). In the present model, this voltage dependence is achieved through the term $\bar{\mu}_\infty$. A function $\bar{\mu}_\infty(V)$ is defined in such a way that the normalized conductance, $c/(\bar{\mu}_\infty(V) + c)$, agrees with the measurements reported in Barrett et al. Then, for a fixed c, the potassium current I_{K2} has voltage dependence similar to the delayed rectifying current I_{K1}.

The variable c included in this model actually represents calcium concentration in the axon hillock region. Experiments have shown, however, that the calcium-activated potassium channels are located in the R_{15} soma proper, not the hillock (Lewis 1988; Lewis et al. 1984). Because the current spreads into the hillock it is included in the model. However, the calcium concentration in the hillock is probably not a true representation of that in the soma. For this reason, somal calcium concentration is fixed at 0.15 μM, within the physiological range established for resting *Aplysia* neurons (Baimbridge et al. 1982). Then, after scaling, the normalized I_{K2} conductance is $1/[\mu_\infty(V) + 1]$, where $\mu_\infty(V) = \bar{\mu}_\infty(V)/(0.15\ \mu\text{M})$. Fixing c in the I_{K2} conductance term is somewhat justified by the finding that the increase in I_{K2} due to calcium ion accumulation during the burst is small (Adams and Levitan 1985).

One final modification is made to this current – rather than modeling the conductance so as to reach its steady state immediately upon change in voltage, a small uniform delay is introduced. Thus, in its final form,

$$I_{K2} = \bar{g}_{K2}(V - V_K)/(\mu + 1) \tag{12}$$

where μ is now a variable satisfying

$$\frac{d\mu}{dt} = [\mu_\infty(V) - \mu]/\tau_\mu \tag{13}$$

and τ_μ is small.

2.2 Subthreshold currents

As least three subthreshold currents exist in the R_{15} hillock. Two of them, I_{NSR} and I_D, drive the bursting oscillation and will be called *burst currents*. The third, I_R, is one of two subthreshold currents strengthened by exogenous application of serotonin. Other subthreshold currents which may exist in the hillock are not included

in the present model because they are not thought to play a major role in either the burst production or serotonin modulation mechanism. Most notable among these is the potassium current I_A (Connor and Stevens 1971; Adams and Benson 1985). This current is not altered by serotonin (Benson and Levitan 1983) and, due to its fast inactivation, does not contribute to burst production.

Burst currents. Both I_{NSR} and I_D have been measured in R_{15} as well as other bursting neurons (Adams et al. 1980; Kramer and Zucker 1985a,b; Adams 1985; Adams and Levitan 1985; Lewis 1988). I_{NSR} is a small calcium current which is slowly inactivated by intracellular calcium ions. It is a subthreshold current because, unlike the spike current I_{Ca}, I_{NSR} is partially activated at voltages as low as -70 mV. I_D is a small nonspecific cation current which activates at voltages above -20 mV and deactivates slowly. The slow deactivation allows the current to sum during the burst, increasing with each voltage spike and decreasing fractionally between spikes. It appears that I_D is generated in response to axonal action potentials which, by an unknown mechanism, results in an increased influx of sodium and calcium ions into the hillock region (Adams and Levitan 1985).

The proposed bursting scenario is shown schematically in Fig. 4. With each action potential I_D is increased and calcium ions flow into the neuron. The increase in I_D reinforces the burst while the increased calcium ion concentration inactivates I_{NSR}, weakening the burst. During the early portion of the burst the increase in I_D is greater than the decrease in I_{NSR}, causing the spike frequency to increase. About midway through the burst, the increase in I_D with each spike is matched by its decay between spikes, while I_{NSR} continues to fall. This results in a decay in spike frequency and the eventual termination of the burst.

During the early interburst I_D will be near its peak value, driving the voltage up to levels just below the spike threshold. As this current decays to near zero, the voltage will move downward to more hyperpolarized levels. This rise and slow decay of voltage is the DAP.

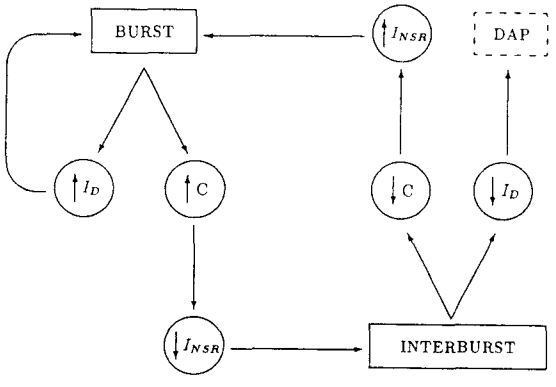

Fig. 4. Schematic illustration of the sequence of events driving the bursting oscillation (flow of events is counterclockwise, starting at the burst)

Since $I_{Ca} \approx 0$ nA during the interburst, the influx of calcium ions is very small. Thus, the intracellular free calcium ion concentration decreases, causing I_{NSR} to lose its inactivation and slowly increase. Eventually I_{NSR} will reach its peak value, which is itself sufficient to induce an action potential and restart the burst.

This scenario accounts for the characteristic parabolic nature of the burst, in which spike frequency is lower at the beginning and end of the burst than during the middle. It also accounts for the DAP, a feature seen in all voltage recordings of bursting R_{15} neurons. Most importantly, it is consistent with known characteristics of the two subthreshold currents.

Due to a lack of detailed data on the kinetics of the burst currents, the model currents used here are developed so as to capture the qualitative behavior of the actual currents. I_{NSR} is modeled as

$$I_{NSR} = \bar{g}_{NSR} q^4 y_\infty(V)(V - V_{Ca}) \tag{14}$$

Activation is brought in through the function $y_\infty(V)$, which varies from zero to one over the interval -70 mV to -5 mV. Slow calcium inactivation is introduced through the factor q^4, where

$$\frac{dq}{dt} = [q_\infty(c) - q]/\tau_q(V) \tag{15}$$

and $q_\infty(c) = 1/(1 + 2c)$. Time constant $\tau_q(V)$ varies from 6 s for $V < -30$ mV to less than 20 ms for $V > 0$ mV. This wide variation allows inactivation to increase proportionally with calcium concentration during the burst and decrease on a slower scale in the interburst interval. The maximum conductance is set to be just large enough to cause the steady-state IV curve, discussed later, to exhibit a region of negative slope.

The model for I_D is

$$I_D = -z \tag{16}$$

where

$$\frac{dz}{dt} = k_z m^3 h - z/\tau_z \tag{17}$$

The first term assures that the current increases with each voltage spike, whereas the second term causes an exponential decay of current between spikes and after the last spike in a burst. Time constant τ_z is chosen large enough to yield slow decay, but smaller than τ_q at hyperpolarized voltages. Parameter k_z is set so that $I_{NSR} + I_D$ is sufficient to induce a second spike after a first one has been initiated. The variables m and h are the I_{Na} activation and inactivation variables, respectively.

Finally, an equation is needed for the rate of change of the intracellular free calcium ion concentration c. The form of the equation used here is fairly standard (Plant 1978; Chay and Keizer 1983), although in this case there are two calcium currents rather than one. The equation is given by

$$\frac{dc}{dt} = -k_i[I_{Ca} + I_{NSR}] - k_e c \tag{18}$$

The influx of free calcium ions is proportional to the two inward calcium currents. The decrease in the concentration of free ions, which may be due primarily to mitochondrial uptake (Smith and Zucker 1980; Chay and Keizer 1983), is approximated here by an exponential decay term $-k_e c$. Smith and Zucker (1980) found that at short times after calcium ion injection the ratio of free to bound ions is about 1:50. This information is used to set the influx parameter k_i. The parameter k_e is set by clamping the model system to -40 mV and requiring that $c \approx 0.1$ μM, a reasonable level for a resting *Aplysia* neuron (Baimbridge et al. 1982).

Inward rectifier. The small potassium current I_R is often referred to as the *inward rectifier* because it is deactivated at most voltages above the potassium equilibrium potential, V_K, but active at voltages below V_K. Thus, it is capable of contributing only a small positive or outward current, but can contribute a large negative or inward current. In most situations I_R adds very little to the total current since voltage does not normally fall below V_K, and although voltage does often enter the region between V_K and -40 mV in which an outward I_R is generated (Drummond et al. 1980; Benson and Levitan 1983), the magnitude of the current produced here is very small.

It has been found that the inward rectifier activates very quickly and does not inactivate (Adams and Benson 1985; Lotshaw et al. 1986), motivating the following model:

$$I_R = \bar{g}_R r_\infty(V)(V - V_K) \tag{19}$$

The infinity function is chosen to be sigmoidal and to vary from 1 to 0 over the interval -110 mV to -40 mV. Maximum conductance is set so that $I_R < 1$ nA for all $V > V_K$, making it almost inconsequential in comparison with the other currents.

2.3 Model bursting

The full R_{15} model consists of ten nonlinear ordinary differential equations (ODEs). The voltage equation is

$$\frac{dV}{dt} = -(I_{spike} + I_{sub} - I_{app})/C_M \tag{20}$$

where

$$I_{spike} = I_{Na} + I_{Ca} + I_{K1} + I_{K2} + I_l \tag{21}$$

$$I_{sub} = I_{NSR} + I_D + I_R \tag{22}$$

Time-dependent behavior of the ionic currents is governed by the remaining ODEs.

The voltage oscillation generated by this model is shown in Fig. 5. Captured here are several characteristic features of the actual oscillation. In particular, a DAP is clearly visible following each burst. In addition, the model burst is parabolic, and the maximum and minimum voltage of each spike grows during the early portion of the burst, a typical feature of the R_{15} oscillation (see Fig. 1). No mechanism has been explicitly built into the model to produce these latter features, thus they are emergent features whose presence builds confidence in the accuracy of the model.

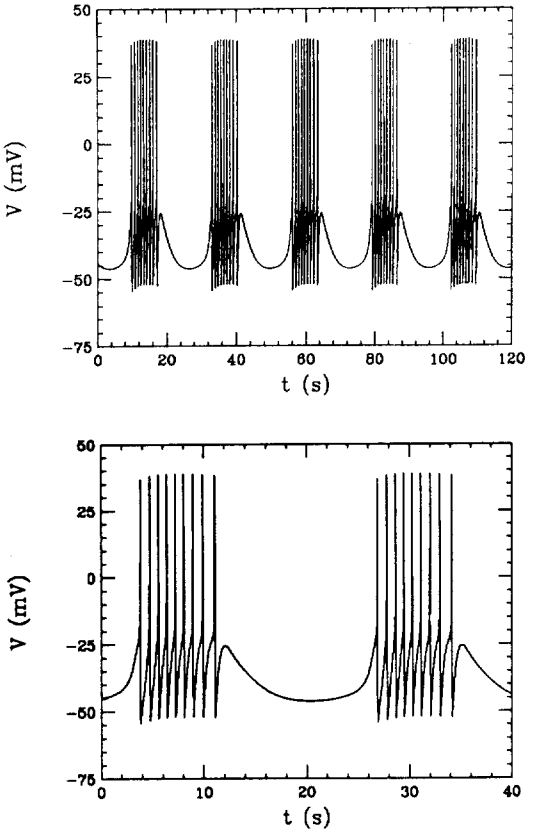

Fig. 5. Model bursting oscillation shown on two different time scales. The system of ordinary differential equations (ODEs) is integrated numerically on a VAX using a Gear method from the IMSL MATH/LIBRARY software package

3 Modeling the effects of serotonin

3.1 Formulation of the serotonin model

As described in the Introduction, exogenous application of serotonin to the soma of R_{15} induces the production of intracellular cyclic AMP which in turn increases the conductance of the two subthreshold currents I_{NSR} and I_R. A relationship between serotonin concentration and change in conductance of the two currents has been established (Drummond et al. 1980; Levitan and Levitan 1988). At low concentration levels (0.1–2 μM) the primary effect is an increase in $\bar{g}_R$. At higher levels (2–10 μM) $\bar{g}_R$ continues to grow while $\bar{g}_{NSR}$ also begins to increase. At still higher concentrations (10–50 μM) no further increase in $\bar{g}_R$ is observed, whereas $\bar{g}_{NSR}$ continues to grow. Thus, $\bar{g}_R$ both increases and saturates earlier than $\bar{g}_{NSR}$.

This information is used to construct a mathematical model in which a dimensionless parameter S is introduced as a measure of serotonin concentration.

Two functions, $\bar{G}_{NSR}(S)$ and $\bar{G}_R(S)$, are then defined for $S \in [0, 1]$ having the following properties:

1. $\bar{G}_{NSR}(0) \approx \bar{g}_{NSR}$, $\bar{G}_R(0) \approx \bar{g}_R$.
2. Both $\bar{G}_{NSR}$ and $\bar{G}_R$ are saturated at $S = 1$.
3. $\bar{G}_{NSR}$ and $\bar{G}_R$ are sigmoidal.
4. $\bar{G}_R$ increases and saturates earlier than $\bar{G}_{NSR}$.

Currents I_{NSR} and I_R are now given by

$$I_{NSR} = \bar{G}_{NSR} q^4 y_\infty(V)(V - V_{Ca}) \quad (23)$$

$$I_R = \bar{G}_R r_\infty(V)(V - V_K) \quad (24)$$

where $\bar{G}_{NSR}(S)$ and $\bar{G}_R(S)$ are illustrated in Fig. 6.

3.2 Steady-state IV curves

A tool often employed by electrophysiologists to study the voltage dependence of ionic currents is the steady-state IV curve. To construct such a curve, the neuron is voltage-clamped at a typically low holding potential until the system reaches equilibrium. It is then clamped to a different potential, the test potential, and the total current recorded after equilibrium is reached. This is repeated for several values of the test potential and the data interpolated to form the IV curve.

This process can be simulated numerically, with the goal of observing the effects of model application of varying concentrations of serotonin on the total ionic current. Figure 7 shows the IV curve at control, when $S = 0$. Subthreshold currents are most important at voltages less than -25 mV, for it is in this range that the initiation of a new spike is determined. Hence, the IV curve is constructed over a range of test voltages below -25 mV.

In this range, the system has a stable equilibrium solution at any point in which the IV curve crosses zero with a positive slope. No such crossing occurs because of a region of negative slope. Indeed, it has been proposed (Wilson and Wachtel 1974) that such a negative slope region (NSR) is necessary for the maintenance of any endogenous neuronal bursting oscillation. The current or currents responsible for the NSR differs from neuron to neuron, but in R_{15} it is I_{NSR} which

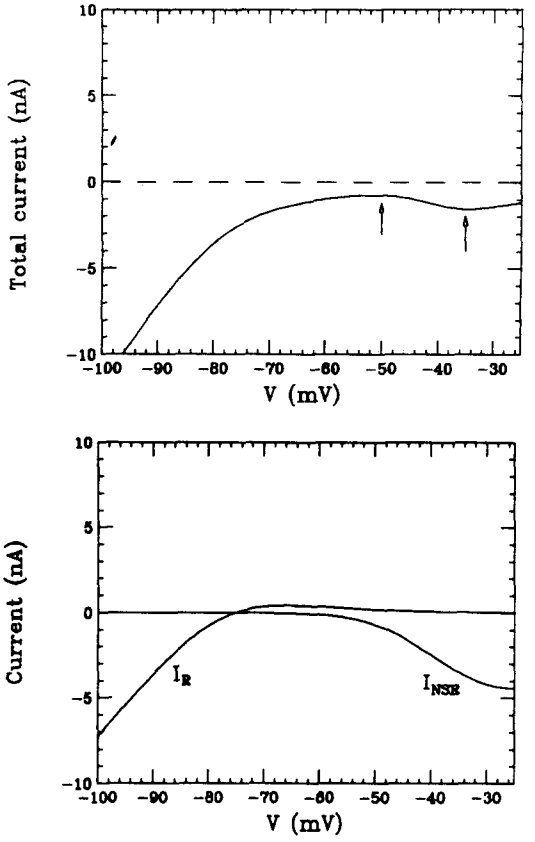

Fig. 7. Model steady-state IV curves for total current (top) and subthreshold currents I_{NSR} and I_R individually (bottom). The negative slope region is located between the arrows. All IV curves were generated by holding V at -70 mV and then pulsing to various test potentials for 1 min

contributes the necessary negative current to prevent the IV curve from crossing zero (Fig. 7, bottom). Also shown in Fig. 7 is I_R, which is largely responsible for the sharp increase in negative current for $V < -75$ mV.

The effect of model application of various concentrations of serotonin on the steady-state IV curve is shown in Fig. 8, where for each of $S = 0.0, 0.3, 0.5, 1.0$

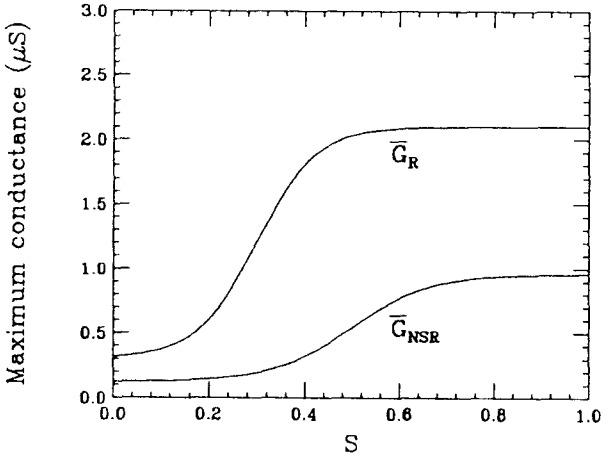

Fig. 6. Dependence of $\bar{G}_{NSR}$ and $\bar{G}_R$ on the serotonin parameter S

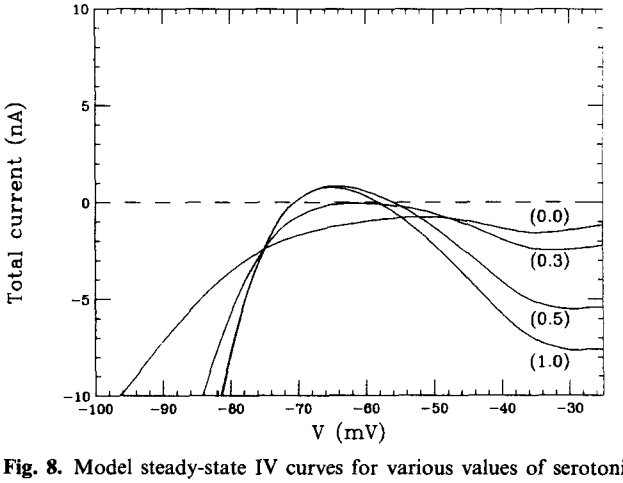

Fig. 8. Model steady-state IV curves for various values of serotonin parameter S

an IV curve is constructed. The curves all intersect at $V_K = -75$ mV, emphasizing that serotonin acts primarily on a potassium current at very low voltages. Due to the increase in I_R, the IV curve becomes more negative at voltages below V_K and more positive at voltages immediately above V_K as S is increased. The increase in I_{NSR} with S causes the IV curve to become more negative at voltages above -50 mV, enhancing the NSR.

With $S = 0.3$ the IV curve comes very close to zero at $V = -60$ mV. Hence, for some parameter value S_1 close to but greater than 0.3, the IV curve will be tangent to the line $I = 0$ at a voltage V_1 near -60 mV. For $S > S_1$ the IV curve will cross zero at two locations, one greater than and the other less than V_1. At the former, the IV curve will have negative slope and thus the crossing will represent an unstable equilibrium point. At the latter the slope of the IV curve is positive, the crossing then representing a stable equilibrium point. The system, therefore, has a stable equilibrium solution for all $S > S_1$.

3.3 Influence of serotonin on the voltage waveform

In Fig. 9 the model waveform is shown for various values of serotonin parameter S. When $S = 0.3$ (Fig. 9b) the number of spikes in a burst is increased from 9 at control (Fig. 9a) to 21. This is due to the increase in the excitatory current I_{NSR}. In addition, the depth and duration of the interburst is greatly increased over control. This is due partly to the increase in the number of spikes per burst, which elevates c during the burst resulting in a more complete inactivation of I_{NSR}. It is also partly due to the increase in I_R which moves the IV curve close to zero for V in the vicinity of -60 mV, slowing the rate of traversal through this region.

The IV curves tell us that a stable stationary or equilibrium point exists at $S = 0.5$ and $S = 1.0$. At $S = 0.5$ this equilibrium is approached asymptotically from any reasonable starting location (Fig. 9c). However, at $S = 1.0$ most trajectories are attracted instead to a periodic beating solution which coexists with the stationary solution (Fig. 9d). In such a beating oscillation the partial inactivation of I_{NSR} is insufficient to terminate the burst.

To examine the solution structure at all values of $S \in [0, 1]$ a bifurcation diagram has been constructed (Fig. 10) using the numerical continuation package AUTO (Doedel 1981) as well as direct time integration. For $S < S_1$, where $S_1 = 0.305$ (to three decimal places), a stable bursting oscillation is present. This oscillation is depicted on the diagram by plotting, for each S less than S_1, the minimum voltage during the interburst.

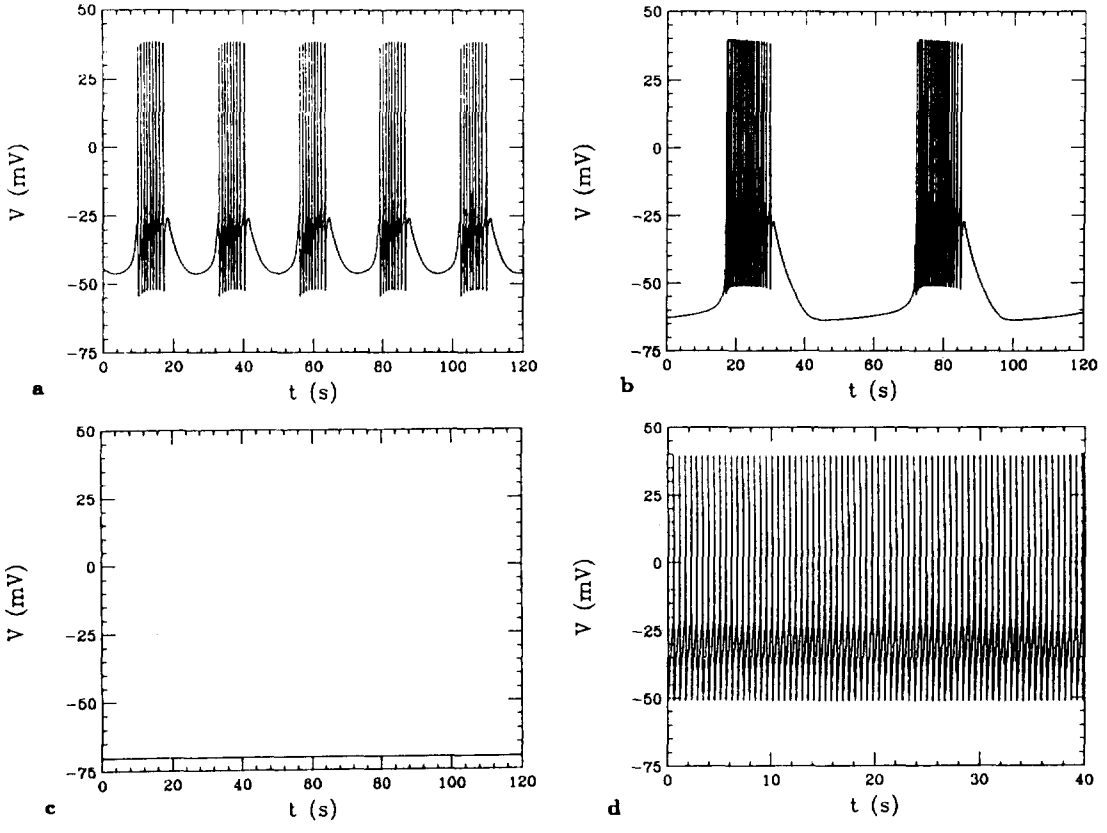

Fig. 9. Simulation of the influence of serotonin on the voltage waveform. **a** $S = 0.0$; **b** $S = 0.3$; **c** $S = 0.5$; **d** $S = 1.0$. Waveform modulation is similar to that seen in the laboratory (Drummond et al. 1980; Levitan and Levitan 1988)

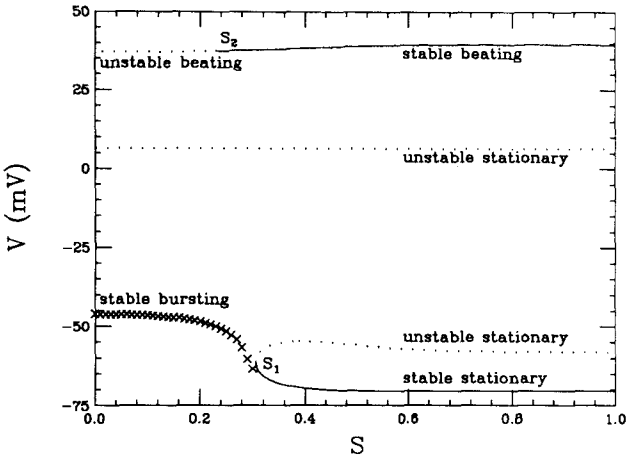

Fig. 10. Bifurcation diagram with bifurcation parameter S. The type and stability of solution branches are labeled. For the bursting branch, the minimum interburst voltage is plotted. For the beating branch, the maximum voltage during one period of oscillation is plotted. A pair of stationary branches is born via saddle node bifurcation at $S = S_1$. The beating branch changes stability via a period doubling bifurcation at $S = S_2$

From the diagram we see that the depth of the interburst increases monotonically as S increases, though the monotonic increase in period is not indicated. The branch of bursting solutions is constructed by numerically integrating the system of ODEs forward in time with S ranging from 0.0 to 0.3.

At $S = S_1$ a stationary solution comes into existence corresponding to the point of tangency of the steady-state IV curve with the line $I = 0$. For $S > S_1$ there will be both a stable and unstable stationary solution corresponding to zero-crossings of the IV curve with positive and negative slope, respectively. In addition, an unstable stationary solution exists for all values of S. This is at a very depolarized voltage and corresponds to a final zero-crossing of the steady-state IV curve. Although the curve crosses zero with a positive slope, the stationary point is unstable, the instability brought on by the fast and largely transient excitatory spike currents which are active at this voltage.

A periodic beating branch arises via Hopf bifurcation from the depolarized unstable stationary branch and is present for all $S \in [0, 1]$. The bifurcation point (not visible in Fig. 10) is reached by setting $S = 1$ and treating I_{app} as the bifurcation parameter. The Hopf bifurcation then occurs at $I_{app} = 8.662$ nA (to three decimal places), and from here the beating branch is traced back down to the $I_{app} = 0$ plane, where S resumes its role as bifurcation parameter.

Stability of the beating solution is lost via period doubling bifurcation at $S = S_2$, where $S_2 = 0.233$ (to three decimal places). The period-doubled branch, not shown in the diagram, emanates subcritically from this point and is thus unstable. Hence, for $S < S_2$ no stable beating solution exists.

For $S_2 < S < S_1$, stable beating and bursting solutions coexist. Since the system was attracted to the bursting oscillation from all physiologically relevant initial conditions tried, it appears that the basin of attraction of the beating solution in the 10-dimensional phase space occupies only a small portion of the region in which the system is found under physiological conditions. For future reference, such as basin is called "small".

Stable beating and stationary solutions coexist for $S_1 < S \leqslant 1.0$. The basin of attraction of the beating solution is small for S near S_1 and large for S near 1.

4 Discussion

Figure 10 aids in the interpretation of the changes through which the R_{15} waveform goes as serotonin concentration is increased. We see from the diagram that for low serotonin concentrations ($S < S_1$) the system should burst, and the depth of the interburst should increase with S. For $S > S_1$ no stable bursting oscillation is present, while stable stationary and beating solutions coexist. For S near S_1 the beating basin is too small to attract trajectories from reasonable starting locations. This basin grows as S increases and at some point, denoted S_3, is large enough to attract trajectories. Hence, at medium serotonin concentrations $S_1 < S < S_3$) the system should asymptotically approach a hyperpolarized stationary solution; that is, it should be found in a quiescent state. For $S > S_3$, trajectories may be attracted to either stable solution, attraction to the beating solution becoming more likely as S is increased. Hence, for large concentrations ($S_3 < S \leqslant 1.0$), the system will generally be found in a beating state. These remarks are summarized in Fig. 11.

Discussion thus far has concerned an R_{15} soma in isolation; that is, the influence of surrounding neurons on the behavior of R_{15} through classic (i.e., nonserotonergic) synaptic coupling has not yet been considered. Such coupling involves, for instance, the neurotransmitters acetylcholine (ACh) or glutamic acid. Coupling involving ACh produces short-term depolarizing perturbations of low magnitude, whereas coupling involving glutamic acid produces similar hyperpolarizing perturbations (Carpenter et al. 1978). What impact would a classic synaptic event (CSE) or perturbation have on the dynamics of the system? From Fig. 10 it is

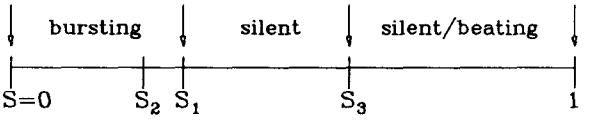

Fig. 11. Summary of voltage response: $S_1 = 0.305$; $S_2 = 0.233$; $S_3 \approx 0.65$. S_1 and S_2 accurate to three decimal places

clear that the answer depends on the concentration of serotonin applied previously. At low concentrations the bursting solution is, for practical purposes, the only attracting solution. Hence, the only long-term effect of a CSE is a resetting of the phase of oscillation. Short-term effects involve the shortening or lengthening of a single burst or interburst (Bertram, manuscript in preparation).

The bistable region $[S_1, 1.0]$ is perhaps more interesting. The hyperpolarized unstable stationary branch acts as a threshold. If, at a given S, the system is perturbed from the stable stationary solution to a point above the hyperpolarized unstable solution, then a burst of action potentials will be generated. The exact number of spikes in the burst depends on S and not on the magnitude of the perturbation.

If $S < S_3$, the burst will be of finite duration, followed by a return to the hyperpolarized stationary state. If $S > S_3$ the burst will be of infinite duration. In this case, a depolarizing voltage perturbation is sufficient to push the system into the basin of attraction of the beating solution.

In Fig. 12 the duration of the burst of spikes following a voltage perturbation to a point above threshold is shown for several values of $S > S_1$. The duration increases with S and is finite for $S \leqslant 0.6$, becoming infinite at $S = 0.65$. This indicates that $0.6 < S_3 < 0.65$.

These results should be interpreted in light of the role played by R_{15} as a secretory cell, releasing osmoregulatory hormone with each spike. At control or after application of low concentrations of serotonin ($S < S_1$) to R_{15}, hormone is secreted periodically with each burst of action potentials, the quantity released being proportional to the duration of the burst. This behavior is not altered by CSEs, which can only reset the phase of oscillation. For this reason, the coupling between the electrical activity of R_{15} and that of surrounding neurons, and hence the coupling between the electrical activity of surrounding neurons and water balance in the animal, is weak.

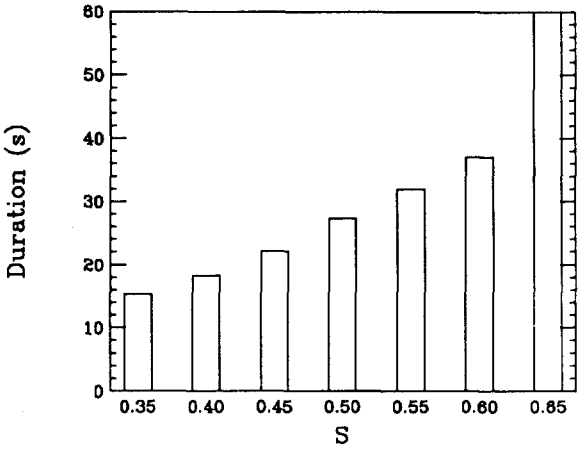

Fig. 12. Duration of the burst following a suprathreshold voltage perturbation for several values of S. The burst duration is insensitive to the magnitude of perturbation, requiring only that it be above threshold. The burst duration at $S = 0.65$ is infinite, indicating that the system has been perturbed into the basin of attraction of the beating solution

At medium concentrations ($S_1 < S < S_3$) the system is at rest, and no hormone is secreted. However, there is now great sensitivity to synaptic perturbations. A sufficiently large event can lead to a transient spiking response lasting for tens of seconds, during which hormone is secreted. In effect, then, the coupling between neurons surounding R_{15} and water balance hasbeen significantly strengthened, while R_{15} itself acts solely as a binary signal transducer.

At large concentrations ($S > S_3$) the neuron may be either silent or in a beating state during which hormone is released continuously. Of course, continuous secretion of hormone assumes intracellular stores will not be depleted, which may not be a valid assumption. In any case, if the cell is in a beating state then it will secrete hormone, and if in a silent state, then a sufficiently large synaptic event can throw the system into a beating state. Again there is a strong coupling between surrounding neurons and water balance.

Appendix: parameters and functions

A.1 Parameters and their values

Parameter	value	parameter	value
C_M	50 nF	I_{app}	0 nA
V_{Na}	55 mV	V_K	−75 mV
V_l	−40 mV	V_{Ca}	100 mV
$\bar{g}_{Na}$	18.0 μS	$\bar{g}_l$	0.07 μS
$\bar{g}_{K1}$	20.0 μS	$\bar{g}_{K2}$	20.0 μS
$\bar{g}_{Ca}$	5.0 μS	$\bar{g}_{NSR}$	0.12 μS
$\bar{g}_R$	0.3 μS	k_z	0.265 nA(ms)$^{-1}$
k_i	4.1 μMC^{-1}(cm)$^{-3}$	k_e	1.22×10^{-4} (ms)$^{-1}$

A.2 Activation/inactivation functions

$$m_\infty(V) = \left\{\frac{\exp[0.26(V-2)]}{1+\exp[0.26(V-2)]}\right\}^{1/3}, \qquad n_\infty(V) = \left\{\frac{\exp[0.22(V-7)]}{1+\exp[0.22(V-7)]}\right\}^{1/2}$$

$$h_\infty(V) = 1/\{1+\exp[(V+12)/3]\}, \qquad j_\infty(V) = 0.4 + 0.6/\{1+\exp[0.26(V+7)]\}$$

$$q_\infty(c) = 1/(1+2c), \qquad y_\infty(V) = 1/\{1+\exp[-0.2(V+35)]\}$$

$$\mu_\infty(V) = \frac{\exp[0.044(67.5-V)]}{0.15(1+\exp[0.044V])}, \qquad r_\infty(V) = 1/\{1+\exp[0.125(V+80)]\}$$

$$x_\infty(V) = \frac{0.1(65-\tilde{V})}{0.1(65-\tilde{V}) + 5\exp[0.1(125-2\tilde{V})] - 5\exp[0.1(60-\tilde{V})]}$$

where $\tilde{V} = (\frac{127}{105})V + (\frac{8265}{105})$

A.3 Time constants (ms)

$$\tau_m(V) = 0.5 + 4.5/\{1+\exp[0.2(V+2)]\}, \qquad \tau_h(V) = 10 + 10/[1+\exp(0.2V)]$$

$$\tau_j(V) = 2000/\{1+\exp[0.2(V-10)]\}, \qquad \tau_q(V) = 1 + 5999/\{1+\exp[0.4(V+15)]\}$$

$$\tau_z = 2000 \qquad \tau_\mu = 2$$

$$\tau_n(V) = \left\{10 + \frac{70}{1+\exp[0.1(V-10)]}\right\} \times \left\{\frac{\exp[0.1(V+35)]}{1+\exp[0.1(V+35)]}\right\}$$

$$\tau_x(V) = \frac{\exp[0.1(65-\tilde{V})] - 1}{0.01(65-\tilde{V}) + 0.5\exp[0.1(125-2\tilde{V})] - 0.5\exp[0.1(60-\tilde{V})]}$$

A4 Serotonin functions (μS)

$$\bar{G}_{NSR}(S) = 0.12 + 0.84/\{1+\exp[-3(5S-3)]\}, \qquad \bar{G}_R(S) = 0.3 + 1.8/\{1+\exp[-1.6(10S-3)]\}$$

Acknowledgements. The author is grateful to Drs. Jerry Magnan and Stuart Dryer for many fruitful discussions and for helpful comments on the manuscript. This work was supported by the Florida State University Supercomputer Computations Research Institute, which is partially funded by the U.S. Department of Energy through contract no. DE-FC05-85ER250000.

References

Adams DJ, Gage PW (1979a) Ionic currents in response to membrane depolarization in an *Aplysia* neurone. J Physiol (Lond) 289:115–141

Adams DJ, Gage PW (1979b) Characteristics of sodium and calcium conductance changes produced by membrane depolarization in an *Aplysia* neurone. J Physiol (Lond) 289:143–161

Adams WB (1985) Slow depolarizing and hyperpolarizing currents which mediate bursting in *Aplysia* neurone R_{15}. J Physiol (Lond) 360:51–68

Adams WB, Benson JA (1985) The generation and modulation of endogenous rhythmicity in the *Aplysia* bursting pacemaker neuron R_{15}. Prog Biophys Mol Biol 46:1–49

Adams WB, Benson JA (1989) Rhythmic neuronal burst generation: experiment and theory. In: Goldbeter A (ed) Cell to cell signalling: from experiments to theoretical models. Academic Press, London, pp 29–45

Adams WB, Levitan IB (1985) Voltage and ion dependences of the slow currents which mediate bursting in *Aplysia* neurone R_{15}. J Physiol (Lond) 360:69–93

Adams WB, Parnas I, Levitan IB (1980) Mechanism of long-lasting synaptic inhibition in *Aplysia* neuron R_{15}. J Neurophysiol 44:1148–1160

Baimbridge KG, Miller JJ, Parkes CO (1982) Calcium-binding protein distribution in the rat brain. Brain Res 239:519–525

Barrett JN, Magleby KL, Pallotta BS (1982) Properties of single calcium-activated potassium channels in cultured rat muscle. J Physiol (Lond) 331:211–230

Benson JA, Levitan IB (1983) Serotonin increases an anomalously rectifying K^+ current in the *Aplysia* neuron R_{15}. Proc Natl Acad Sci USA 80:3522–3525

Byerly L, Hagiwara S (1982) Calcium currents in internally perfused nerve cell bodies of *Limnaea stagnalis*. J Physiol (Lond) 322:503–528

Canavier CC, Clark JW, Byrne JH (1991) Simulation of the bursting activity of neuron R15 in Aplysia: role of ionic currents, calcium balance, and modulatory transmitters. J Neurophysiol 66:2107–2124

Carpenter DO, McCreery MJ, Woodbury CM, Yarowsky PJ (1978) Modulation of endogenous discharge in neuron R_{15} through specific receptors for several transmitters. In: Chalazonitis N, Boisson M (eds) Abnormal neuronal discharges. Raven Press, New York, pp 189–203

Chay TR, Keizer J (1983) Minimal model for membrane oscillations in the pancreatic β-cell. Biophys J 42:181–190

Connor JA, Stevens CF (1971) Prediction of repetitive firing behavior from voltage clamp data on an isolated neurone soma. J Physiol (Lond) 213:31–53

Doedel EJ (1981) AUTO: a program for the automatic bifurcation and anslysis of autonomous systems. Congr Numerantium 30:265–284

Drummond AH, Benson JA, Levitan IB (1980) Serotonin-induced hyperpolarization of an identified *Aplysia* neuron is mediated by cyclic AMP. Proc Natl Acad Sci USA 77:5013–5017

Gorman ALF, Thomas MV (1980) Potassium conductance and internal calcium accumulation in a molluscan neurone. J Physiol (Lond) 308:287–313

Gorman ALF, Hermann A, Thomas MV (1982) Ionic requirements for membrane oscillations and their dependence on the calcium concentration in a molluscan pace-maker neurone. J Physiol (Lond) 327:185–217

Hille B (1984) Ionic channels of excitable membranes. Sinauer Associates, Sunderland, Mass

Hindmarsh JC, Rose RM (1984) A model of neuronal bursting using three coupled first order differential equations. Proc R Soc Lond [Biol] 221:87–102

Hodgkin AL, Huxley AF (1952) A quantitative description of membrane current and its application to conduction and excitation in nerve. J Physiol (Lond) 117:500–544

Junge D, Stephens CL (1973) Cyclic variation of potassium conductance in a burst-generating neurone in *Aplysia*. J Physiol (Lond) 235:155–181

Kandel ER (1979) Behavioral biology of *Aplysia*. Freeman, San Francisco, p 324

Kramer RH, Zucker RS (1985a) Calcium-dependent inward current in *Aplysia* bursting pace-maker neurones. J Physiol (Lond) 362:107–130

Kramer RH, Zucker RS (1985b) Calcium-induced inactivation of calcium current causes the inter-burst hyperpolarization of *Aplysia* bursting neurones. J Physiol (Lond) 362:131–160

Levitan ES, Levitan IB (1988) Serotonin acting via cyclic AMP enhances both the hyperpolarizing and depolarizing phases of bursting pacemaker activity in the *Aplysia* neuron R_{15}. J Neurosci 8:1152–1161

Levitan ES, Kramer RH, Levitan IB (1987) Augmentation of bursting pacemaker activity by egg-laying hormone in *Aplysia* neuron R_{15} is mediated by a cyclic AMP-dependent increase in Ca^{2+} and K^+ currents. Proc Natl Acad Sci USA 84:6307–6311

Lewis DV (1984) Spike aftercurrents in R_{15} of *Aplysia*: their relationship to slow inward current and calcium influx. J Neurophysiol 51:387–403

Lewis DV (1988) Calcium-activated inward spike after-currents in bursting neurone R_{15} of *Aplysia*. J Physiol (Lond) 395:285–302

Lewis DV, Evans GB, Wilson WA (1984) Dopamine reduces slow outward current and calcium influx in burst-firing neuron R_{15} of *Aplysia*. J Neurosci 4:3014–3020

Lotshaw DP, Levitan ES, Levitan IB (1986) Fine tuning of neuronal electrical activity: modulation of several ion channels by intracellular messengers in a single identified nerve cell. J Exp Biol 124:307–322

Mathieu PA, Roberge FA (1971) Characteristics of pacemaker oscillations in *Aplysia* neurons. Can J Physiol Pharmacol 49: 787–795

Mayeri E, Rothman BS, Brownell PH, Branton WD, Padgett L (1985) Nonsynaptic characteristics of neurotransmission mediated by egglaying hormone in the abdominal ganglion of *Aplysia*. J Neurosci 5:2060–2077

Plant RE (1978) The effects of calcium^{++} on bursting neurons. Biophys J 21:217–237

Plant RE, Kim M (1975) On the mechanism underlying bursting in the *Aplysia* abdominal ganglion R_{15} cell. Math Biosci 26:357–375

Rinzel J, Lee YS (1987) Dissection of a model for neuronal parabolic bursting. J Math Biol 25:653–675

Smith TG (1980) Ionic conductances in bursting pacemaker cells and their hormonal modulation. In: Koester J, Byrne JH (eds) Molluscan nerve cells: from biophysics to behavior. Cold Spring Harbor Laboratory, Cold Spring Harbor, NY, pp 135–143

Smith SJ, Zucker RS (1980) Aequorin response facilitation and intracellular calcium accumulation in molluscan neurones. J Physiol (Lond) 300:167–196

Thompson SH (1977) Three pharmacologically distinct potassium channels in molluscan neurons. J Physiol (Lond) 265: 465–488

Wilson WA, Wachtel H (1974) Negative resistance characteristic essential for the maintenance of slow oscillations in bursting neurons. Science 186:932–934

Note added in proof. A previous computational study of some of the effects of serotonin on R_{15} is discussed in Canavier et al. (1991).